Using exact relations in damage-spreading simulations: The Baxter line of the two-dimensional Ashkin-Teller model

A. S. Anjos,[1,*] D. A. Moreira,[1,†] A. M. Mariz,[1,‡] F. D. Nobre,[2,§] and F. A. da Costa[1,‖]
[1]*Departamento de Física Teórica e Experimental, Universidade Federal do Rio Grande do Norte, Campus Universitário, Caixa Postal 1641, 59072-970, Natal, Rio Grande do Norte, Brazil*
[2]*Centro Brasileiro de Pesquisas Físicas, Rua Xavier Sigaud 150, 22290-180, Rio de Janeiro, Brazil*
(Received 24 April 2007; revised manuscript received 17 September 2007; published 29 October 2007)

The nearest-neighbor-interaction ferromagnetic Ashkin-Teller model is investigated on a square lattice through a powerful computational method for dealing with correlation functions in magnetic systems. This technique, which is based on damage-spreading numerical simulations, makes use of exact relations involving special kinds of damage and correlation functions, as well as the corresponding order parameters of the model. The computation of correlation functions, which represents usually a hard task in standard Monte Carlo simulations, due to large fluctuations, turns out to be much simpler within the present approach. We concentrate our analysis along the Baxter line, well known for its continuously varying critical exponents; seven different points along this line are investigated. The critical exponents associated with correlation functions along the Baxter line are successfully evaluated, by means of numerical methods, within damage-spreading simulations. The efficiency of this method is confirmed through precise estimates of the critical exponents associated with the order parameters (magnetization and polarization), as well as with their corresponding correlation functions, in spite of the small lattice sizes considered.

DOI: 10.1103/PhysRevE.76.041137 PACS number(s): 05.50.+q, 05.10.Ln, 64.60.Fr, 75.10.Hk

I. INTRODUCTION

Since its introduction, the Ashkin-Teller model [1] has attracted the attention of many researchers; the predominantly investigated version has been the ferromagnetic model on a square lattice (see, e.g., Refs. [2–10]). One of the most striking features of this model occurs along the so-called Baxter line [2,3], where *universality is broken*; i.e., some critical exponents may change continuously by a simple variation of the parameters of the system, like temperature and couplings. The dependence of these critical exponents on such parameters was determined analytically for the whole line [3,11], which includes two well-known points: namely, the Ising and four-state Potts points. Therefore, the Baxter line represents a very appropriate locus for testing the accuracy of any method proposed for computing critical exponents approximately.

Recent advances in computer technology have produced a great burst of interest in many approximative methods of statistical mechanics. In particular, computer simulations [12] became one of the most powerful tools for studying physical systems; among these, one may single out the Monte Carlo (MC) method [13,14] as a commonly-used technique, being applied successfully to a wide variety of systems. In a standard MC simulation one is particularly interested in the dynamical (i.e., out-of-equilibrium) behavior or in the long-time (presumably at equilibrium) properties of a given physical system. In this case, one follows the time evolution of a single copy of the system, with the dynamical variables being updated according to certain dynamical rules. Since one has to deal with finite systems, finite-size effects represent a major drawback in this procedure, in such a way that one is always obliged to simulate the largest possible sizes, taking into consideration the computing facilities available.

A very effective type of MC simulation, for studying both dynamical and static properties of statistical models, is known as the "damage-spreading" (DS) technique [15,16]. In this case, one investigates the time evolution of the Hamming distance between two (originally identical) copies of a given system, given that a perturbation (or damage) is introduced in one of them at the initial time. The two copies should evolve under the same updating rules and sequences of random numbers, in such a way as to guarantee that the possible differences between the two copies, at later times, should be due only to their initial damage. In order to investigate their dynamic properties, the DS method has been applied to many magnetic systems, like the Ising [15–21] and Potts [22–25] models, among others. One of the intriguing aspects in such investigations was that the propagation of the initial damage depended on the particular dynamical procedure used for the simulations.

A major breakthrough occurred when exact relations involving quantities computable from DS simulations and thermodynamic properties were derived for the Ising ferromagnet, leading to the possibility of a new numerical procedure to estimate quantities like order parameters and two-spin correlation functions [26]. Subsequently, similar exact relations were derived also for more complicated systems, like the Potts [27], Ashkin-Teller [27], discrete N-vector [28], and (N_α, N_β) [29] models. These relations are valid for translationally invariant systems and hold for any ergodic dynamical procedure, leading to thermodynamic properties that do

*asafilho@dfte.ufrn.br
†darlan@dfte.ufrn.br
‡ananias@dfte.ufrn.br
§Corresponding author. fdnobre@cbpf.br
‖fcosta@dfte.ufrn.br

not depend on the particular kind of dynamics employed, as expected. Their implementation in numerical simulations was done, as an illustrative example, for the ferromagnetic Ising model on a square lattice [26], resulting in a significant reduction of finite-size effects. Recently, the corresponding relations for the Potts model were applied in simulations of the q-state Potts ferromagnet on a square lattice [30]. The efficiency of the method was illustrated through precise estimates of the critical exponents β and η, associated, respectively, with the magnetization and two-spin correlation function, for $q=2$, 3, and 4, notwithstanding the small lattice sizes used. In particular, the fluctuations that usually come out very strong in the computation of the two-spin correlation function, within standard MC simulations, appeared to be much inhibited through the DS simulations of the Potts model [30].

In the present work we investigate the ferromagnetic Ashkin-Teller model through DS simulations by using the exact relations derived in Ref. [27]. Our analysis is restricted to the Baxter line; the effectiveness of the method is confirmed herein through precise estimates of the critical exponents associated with the order parameters of the system, as well as with their associated correlation functions. In the next section, we define the numerical procedure and in Sec. III we present and discuss our results.

II. MODEL AND NUMERICAL PROCEDURE

The Ashkin-Teller model [1] may be defined in terms of two Ising variables at each site of a regular lattice. In the present work we shall consider the Ashkin-Teller ferromagnet on a square lattice of linear dimension L ($N=L^2$ is the total number of spins), defined through the Hamiltonian

$$\mathcal{H} = \sum_{\langle ij \rangle} [-J_1(\sigma_i\sigma_j + \tau_i\tau_j) - 2J_2(\sigma_i\sigma_j\tau_i\tau_j)] \quad (\sigma_i, \tau_i = \pm 1), \tag{1}$$

with $J_1 \geq 0$ and $J_1 + 2J_2 \geq 0$, whereas the summation $\Sigma_{\langle ij \rangle}$ runs over all pairs of nearest-neighbor sites. Two particular cases may be obtained easily from the above Hamiltonian—i.e., $J_2=0$ (two independent Ising models) and $J_1=2J_2$ (four-state Potts model).

The phase diagram of this model is quite well known due to various theoretical investigations [2–9]; it is presented in Fig. 1 in terms of the thermal transmissivities (t_1, t_2) [9],

$$t_1 = \frac{1 - \exp(-4K_1)}{1 + 2\exp[-2(K_1 + 2K_2)] + \exp(-4K_1)}, \tag{2a}$$

$$t_2 = \frac{1 - 2\exp[-2(K_1 + 2K_2)] + \exp(-4K_1)}{1 + 2\exp[-2(K_1 + 2K_2)] + \exp(-4K_1)}, \tag{2b}$$

where $K_1=J_1/(k_BT)$ and $K_2=J_2/(k_BT)$. Solid lines represent critical frontiers separating the three possible phases of the model, which are defined in terms of the relevant order parameters—i.e., the magnetizations $\langle\sigma\rangle$ and $\langle\tau\rangle$, as well as the polarization $\langle\sigma\tau\rangle$, as described below [in fact, due to the symmetry of the Hamiltonian of Eq. (1), this model is characterized by two order parameters only, since $\langle\sigma\rangle=\langle\tau\rangle$].

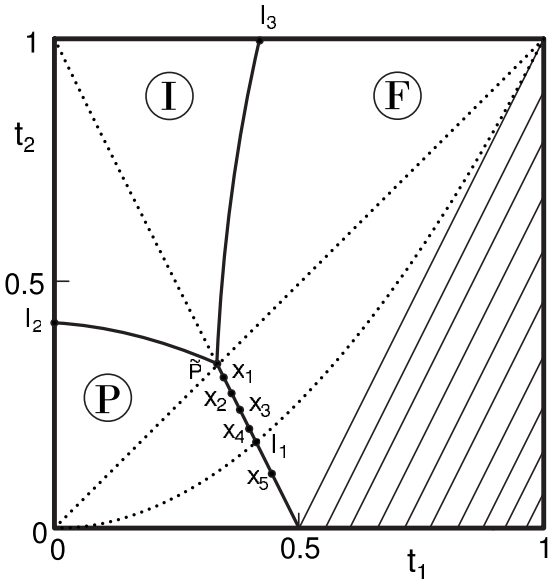

FIG. 1. Phase diagram of the nearest-neighbor-interaction Ashkin-Teller ferromagnet on a square lattice in the (t_1, t_2) space. Three phases are present: namely, the paramagnetic (**P**), ferromagnetic (**F**), and intermediate (**I**). The shaded region is nonphysical [9].

(a) *Paramagnetic* (**P**). The temperature is sufficiently high in such a way that there is no order at all—i.e., $\langle\sigma\rangle=\langle\tau\rangle=\langle\sigma\tau\rangle=0$.

(b) *Ferromagnetic* (**F**). The couplings are sufficiently strong, leading to nonzero order parameters $\langle\sigma\rangle=\langle\tau\rangle\neq 0$ and $\langle\sigma\tau\rangle\neq 0$.

(c) *Intermediate* (**I**). This type of ordering appears only for $J_2 > J_1/2$, characterized by $\langle\sigma\rangle=\langle\tau\rangle=0$ and $\langle\sigma\tau\rangle\neq 0$.

The dotted lines $t_2=t_1^2$ $(J_2=0)$ and $t_1=t_2$ $(J_1=2J_2)$ correspond to special subspaces associated with two independent Ising models and the four-state Potts model, respectively. The dotted straight line $t_2=1-2t_1$ is self-dual, and part of it constitutes the critical frontier separating the phases **P** and **F**. The intersection of the Ising and four-state Potts lines with the critical frontier **P**-**F** yields the Ising (I_1) and four-state Potts $(\tilde{P})$ critical points, as shown in Fig. 1. At the Potts critical point, the critical frontier **P**-**F** bifurcates in two critical frontiers, separating the phases **F** and **I**, as well as **P** and **I**. The critical frontiers **P**-**I** and **I**-**F** are related to each other by duality and belong to the Ising universality class [8,9], dominated by their respective end points I_2 and I_3. In the phase diagram of Fig. 1, the critical frontier **P**-**F** is known as the Baxter line [2,3,11], characterized by continuously varying critical exponents.

The present analysis is concerned with the computation of the critical exponents associated with correlation functions and order parameters for several points along the Baxter line, using, jointly, DS simulations and exact relations. The DS technique consists in the investigation of the time evolution of two copies of the system, for a given temperature T, sub-

jected to the same thermal noise and same set of random numbers. For the Ashkin-Teller model, these copies (denoted herein by A and B) are represented in terms of two Ising variables at each site of the lattice, $\{\sigma_i^A, \tau_i^A\}$ and $\{\sigma_i^B, \tau_i^B\}$. In the DS simulation, first of all, we let one copy (e.g., $\{\sigma_i^A, \tau_i^A\}$) evolve for t_{eq} MC steps toward equilibrium; as usual, our unit of time (1 MC step) consists in a complete sweep of the lattice. We assume that the equilibrium state is attained when one observes small fluctuations in time on thermodynamic quantities, like magnetization and energy; in addition to that, we have also checked such an equilibrium state by a comparison of some DS quantities, to be defined below. Then, one defines the initial time ($t=0$), at which the second copy (copy B) is created by replicating copy A; at this time, one introduces certain modifications in copy B, corresponding to the initial damage. Copies A and B will then evolve in time according to some ergodic dynamics, subject to certain boundary conditions, as imposed by the corresponding exact relations to be used. Such exact relations involve certain time averages computable from DS numerical simulations and thermodynamic properties of the Ashkin-Teller model [27]. It is important to mention that these relations hold for any ergodic dynamics applied to translationally invariant systems.

Let us then define the DS quantities

$$\Gamma_i^{(1)} = \frac{1}{2}\langle 1 + \sigma_i^A \rangle_t - \frac{1}{2}\langle 1 + \sigma_i^B \rangle_t, \tag{3a}$$

$$\Omega_i^{(1)} = \frac{1}{2}\langle 1 + \tau_i^A \rangle_t - \frac{1}{2}\langle 1 + \tau_i^B \rangle_t, \tag{3b}$$

$$\Gamma_i^{(2)} = \frac{1}{2}\langle 1 + \sigma_i^A \tau_i^A \rangle_t - \frac{1}{2}\langle 1 + \sigma_i^B \tau_i^B \rangle_t, \tag{3c}$$

where $\langle \cdots \rangle_t$ represents time averages over trajectories in phase space. One should stress that, due to the symmetry of the Hamiltonian of Eq. (1), after a long-time numerical simulation (which represents the physical situation of interest in the present work) one expects to get $\Gamma_i^{(1)} = \Omega_i^{(1)}$; in fact, we have also used this condition as an additional criterion for checking the approach to the equilibrium state. Therefore, from now on, we will be concerned only with the quantities $\Gamma_i^{(1)}$ and $\Gamma_i^{(2)}$.

In order to obtain exact relations involving the quantities of Eqs. (3a)–(3c) and correlation functions, as well as order parameters, of the Ashkin-Teller model, we will impose certain constraints (i.e., boundary conditions), either to one of the copies (A or B) or to both of them. Such relations are derived by making use of conditional probabilities that depend on the particular constraints used [27]; therefore, different boundary conditions will lead to different time evolutions, and consequently, in the long-time limit, they will correspond to distinct exact relations, as described below.

(Ia) First, we consider a boundary condition for the variable σ_i^B at the central site of the lattice, $\sigma_0^B = -1$, for all times $t \geq 0$. This represents a "source of damage" at the central site; all remaining spins of the lattice, on both copies, are let free to evolve following the corresponding dynamical procedure. In this case, one may define the binary variable [27] $\Pi_i^\sigma = [(1+\sigma_i)/2]$ in such a way that

$$\langle \Pi_i^{\sigma,A} \rangle_t = \langle \Pi_i^\sigma \rangle_T,$$

$$\langle \Pi_i^{\sigma,B} \rangle_t = \frac{\langle (1 - \Pi_0^\sigma)\Pi_i^\sigma \rangle_T}{\langle 1 - \Pi_0^\sigma \rangle_T},$$

and now $\langle \cdots \rangle_T$ stands for thermal averages. In the equations above, $\langle \Pi_i^{\sigma,A} \rangle_t$ represents the probability for the variable σ_i^A presenting the value +1 with no restrictions, whereas $\langle \Pi_i^{\sigma,B} \rangle_t$ is the conditional probability for finding the variable $\sigma_i^B = 1$, provided that $\sigma_0^B = -1$. In addition to that, we are assuming that our system is translationally invariant and that it evolves in time under an ergodic dynamics. Since

$$\Gamma_i^{(1)} = \langle \Pi_i^{\sigma,A} \rangle_t - \langle \Pi_i^{\sigma,B} \rangle_t,$$

one gets that

$$\Gamma_i^{(1)} = \frac{C_{0i}^{(1)}}{2(1-m)}, \tag{4}$$

where

$$C_{0i}^{(1)} = \langle \sigma_i \sigma_0 \rangle_T - \langle \sigma_i \rangle_T \langle \sigma_0 \rangle_T, \tag{5a}$$

$$m = \langle \sigma_0 \rangle_T. \tag{5b}$$

Since we are supposing translational invariance, the quantities above represent standard thermodynamic quantities: namely, the two-spin correlation function and magnetization per site, respectively.

(Ib) Now, if one uses a boundary condition for the central sites of both copies A and B—i.e., $\sigma_0^A = 1$ and $\sigma_0^B = -1$—for all times $t \geq 0$, one gets that

$$\Gamma_i'^{(1)} = \frac{C_{0i}^{(1)}}{1 - m^2}. \tag{6}$$

It is important to mention that $\Gamma_i^{(1)}$ and $\Gamma_i'^{(1)}$ are both given by the same expression in Eq. (3a), although they should be computed through different evolution procedures.

Therefore, after the equilibration process of copy A (time $t=0$), this configuration is stored (as a new copy A_0), which will remain untouched; then, the time evolution with the constraint in (Ia) is performed for copies A and B in such a way that one obtains, after t_{av} MC steps, $\Gamma_i^{(1)}$. Now, recovering configuration A_0, which will become configuration A for the time evolution with the constraint in (Ib), one performs such an evolution in order to get $\Gamma_i'^{(1)}$. From these two quantities, using Eqs. (4) and (6), one obtains $C_{0i}^{(1)}$ and m.

Similar relations also hold for the quantity involving the two spins σ and τ—i.e., $\Gamma_i^{(2)}$—as described below.

(IIa) Considering the boundary condition $\sigma_0^B = -\tau_0^B$ ($t \geq 0$), one gets

$$\Gamma_i^{(2)} = \frac{C_{0i}^{(2)}}{2(1-p)}, \tag{7}$$

where

$$C_{0i}^{(2)} = \langle \sigma_i \tau_i \sigma_0 \tau_0 \rangle_T - \langle \sigma_i \tau_i \rangle_T \langle \sigma_0 \tau_0 \rangle_T, \tag{8a}$$

$$p = \langle \sigma_0 \tau_0 \rangle_T. \tag{8b}$$

Again, assuming translational invariance, the quantity $C_{0i}^{(2)}$ represents a different two-point correlation function of the Ashkin-Teller model, whereas the parameter p is usually denominated the "polarization" order parameter [11].

(IIb) The boundary conditions $\sigma_0^A = \tau_0^A$ and $\sigma_0^B = -\tau_0^B$ $(t \geq 0)$ yield

$$\Gamma_i'^{(2)} = \frac{C_{0i}^{(2)}}{1 - p^2}, \tag{9}$$

where, as before, $\Gamma_i^{(2)}$ and $\Gamma_i'^{(2)}$ are given by the same expression [cf. Eq. (3c)], but should be computed with different boundary conditions. By considering two time evolutions following, respectively, the constraints specified in (IIa) and (IIb), a procedure similar to the one described for the cases (Ia) and (Ib) may be applied in order to obtain $C_{0i}^{(2)}$ and p.

In contrast to the results of Ref. [26], the exact relations above do not depend on the "Hamming distance" between two configurations and are written in terms of quantities that are independent of the particular dynamical rule; therefore, these relations hold for any ergodic dynamical procedure. Herein, we have carried numerical simulations, for each configuration, by visiting all sites of the lattice in a sequential way, with the spin variables $\sigma_i^\mu(t)$ and $\tau_i^\mu(t)$ $(\mu = A, B)$, at time t, updated according to the set of dynamical rules described below.

(i) A possible flip in the variable $\sigma_i^\mu(t+1)$ is considered—i.e., $\sigma_i^\mu(t+1) = -\sigma_i^\mu(t)$—from which one calculates the change in energy, $\Delta\mathcal{H}^\mu = \mathcal{H}^\mu(t+1) - \mathcal{H}^\mu(t)$.

(ii) Then, one defines the probability

$$p_i^\mu(t) = \frac{1}{1 + \exp(\beta \Delta \mathcal{H}^\mu)} \quad [\beta = 1/(k_B T)]. \tag{10}$$

(iii) By introducing a random number $z_i^{(\sigma)}(t)$, uniformly distributed in the interval [0,1], one performs the change if $z_i^{(\sigma)}(t) < p_i^\mu(t)$; otherwise, the spin $\sigma_i^\mu(t)$ is not updated. It should be noticed that, at this step, the same random number $z_i^{(\sigma)}(t)$ is used for the updating of the variable $\sigma_i^\mu(t)$ in both copies A and B.

(iv) Steps (i)–(iii) are repeated for the variable $\tau_i^\mu(t)$, now using a different random number $z_i^{(\tau)}(t)$.

(III) Finally, there is an alternative way to obtain the order parameters m and p by considering copies A and B in the presence of external magnetic fields $h_{i\sigma}^\mu$ and $h_{i\tau}^\mu$ $(\mu = A, B)$; these are dimensionless quantities—i.e., $h_{i\sigma}^\mu = H_{i\sigma}^\mu/(k_B T)$ and $h_{i\tau}^\mu = H_{i\tau}^\mu/(k_B T)$. In this case, after the equilibration of copy A, one starts at time $t=0$ by defining copy B in such a way that $\sigma_i^A = -\sigma_i^B$ and $\tau_i^A = \tau_i^B$ $(\forall\ i)$. Then, all the spins are free to evolve in time under the presence of the magnetic fields $h_{i\sigma}^A = -h_{i\sigma}^B = h$ and $h_{i\tau}^A = h_{i\tau}^B = h$. In this case, the order parameters of the Ashkin-Teller model may be obtained directly from the DS quantities $\Gamma_i^{(1)}$ and $\Gamma_i^{(2)}$ [27],

TABLE I. Coordinates of the critical points shown in the phase diagram of Fig. 1 in both variables (t_1, t_2) and (K_1, K_2). The points I_1, $\widetilde{P}$, and $X_1, \ldots, X_5$ are all along the Baxter line.

Point	t_{1C}	t_{2C}	K_{1C}	K_{2C}
I_1	$\sqrt{2}-1$	$(\sqrt{2}-1)^2$	$-\frac{1}{4}\ln(3-2\sqrt{2})$	0
I_2	0	$\sqrt{2}-1$	0	$-\frac{1}{4}\ln(\sqrt{2}-1)$
I_3	$\sqrt{2}-1$	1	$-\frac{1}{4}\ln(\sqrt{2}-1)$	∞
$\widetilde{P}$	1/3	1/3	$\frac{1}{4}\ln 3$	$\frac{1}{8}\ln 3$
X_1	8/23	7/23	$\frac{1}{4}\ln(23/7)$	$\frac{1}{4}\ln[(\sqrt{161})/8]$
X_2	4/11	3/11	$\frac{1}{4}\ln(11/3)$	$\frac{1}{4}\ln[(\sqrt{33})/4]$
X_3	8/21	5/21	$\frac{1}{4}\ln(21/5)$	$\frac{1}{4}\ln[(\sqrt{105})/8]$
X_4	2/5	1/5	$\frac{1}{4}\ln 5$	$-\frac{1}{4}\ln[(2\sqrt{5})/5]$
X_5	4/9	1/9	$\frac{1}{4}\ln 9$	$\frac{1}{4}\ln(3/4)$

$$m = \langle \sigma_i \rangle_T = \Gamma_i^{(1)}, \quad p = \langle \sigma_i \tau_i \rangle_T = \Gamma_i^{(2)}. \tag{11}$$

In this case, the spin-updating procedure is similar to the one described above, but now the energy change $\Delta\mathcal{H}'^\mu = \mathcal{H}'^\mu(t+1) - \mathcal{H}'^\mu(t)$ should be considered by taking the Hamiltonian of Eq. (1) in the presence of the corresponding external magnetic fields.

The two-site correlation functions in Eqs. (5a) and (8a) take into account the central site of the lattice and an arbitrary site i, a distance r apart. It should be stressed that, on a square lattice, there are four sites i with the same distance r from the central site (with a few exceptions; e.g., if one assumes a unit lattice spacing, one has 8 sites whose distance to the central site is $\sqrt{5}$ and 12 sites for which this distance is 5). Therefore, it is always possible to define the correlation functions as the average values

$$C^{(1)}(r) = \frac{1}{4}\sum_{i(r)} C_{0i}^{(1)}, \quad C^{(2)}(r) = \frac{1}{4}\sum_{i(r)} C_{0i}^{(2)}, \tag{12}$$

where $\Sigma_{i(r)}$ corresponds to a summation over four sites with the same distance r from the central site; in the exceptional cases where there are more than four sites with the same distance r from the central site, the remaining sites are not taken into account in the averages of Eq. (12).

In the next section we present and discuss the results obtained for the magnetization m and polarization p per site, as well as for the correlation functions $C^{(1)}(r)$ and $C^{(2)}(r)$, along the Baxter line of the Ashkin-Teller model.

III. RESULTS AND DISCUSSION

We investigated the Ashkin-Teller ferromagnet on a square lattice of linear dimensions $L=50$ and 100 within the DS framework described above. Periodic boundary conditions were used, and the distance r, in the correlation functions $C^{(1)}(r)$ and $C^{(2)}(r)$, was measured with respect to the central site, located at coordinates $(L/2, L/2)$. Seven different points along the Baxter line were investigated: namely, the Ising (I_1) and four-state Potts $(\widetilde{P})$ points, as well as five additional points—i.e., $X_1, \ldots, X_5$ (see Fig. 1 and Table I).

We have always started copy A with all spins $\sigma_i^A=\tau_i^A=1$ $(\forall\ i)$; then, this copy was let to evolve toward equilibration for $t_{\rm eq}$ MC steps, after which, the second copy (copy B) was created. In the case of the evolution of type (III), where external magnetic fields are necessary, we have attributed small positive numbers to the dimensionless quantity h; in order to find its appropriate value, this quantity was successively decreased in such a way as to find no dependence of the particular choice of the magnetic fields on our results, taking into account the error bars. In the present simulations we have considered $h=0.0001$. For the evolution toward equilibrium, some of the points investigated required larger equilibration times and the maximum equilibration times used were $t_{\rm eq}=1\times10^4$ $(L=50)$ and $t_{\rm eq}=4\times10^4$ $(L=100)$ MC steps. In all simulations considered, these times were sufficient for a fulfillment of the equilibrium conditions described above—i.e., small fluctuations in the magnetization and energy, as well as in the equality $\Gamma_i^{(1)}=\Omega_i^{(1)}$. In the computation of correlation functions, the thermal averages were carried over times $t_{\rm av}=7.5\times10^5$ $(L=50)$ and $t_{\rm av}=3\times10^6$ $(L=100)$ MC steps, whereas in calculation of the order parameters [evolution of type (III)] smaller times were necessary—i.e., $t_{\rm av}=7.5\times10^4$ $(L=50)$ and $t_{\rm av}=3\times10^5$ $(L=100)$ MC steps. It is important to stress that, due to large fluctuations, the times $t_{\rm av}$ considered herein are much larger than those used in simpler ferromagnetic models [26,30]. In order to reduce the possible effects of correlations in time, we only consider, in our time averages, data at each time interval of three MC steps. Therefore, each time average consists in an average over $t_{\rm av}/3$ measurements. In addition to that, each simulation was repeated for $M=20$ different samples, in order to improve the statistics, as well as to reduce possible dependence on sequences of random numbers.

The Baxter line [2,3,11], which coincides with the critical frontier **P**-**F** in the phase diagram of Fig. 1, is well known for its continuously varying critical exponents, and its dependence in terms of the parameters of the phase diagram is well known (see, e.g., Ref. [11] for their dependence on K_1 or Ref. [3] for the exponents in terms of K_2). Below, we write their dependence in terms of K_2; for the specific-heat critical exponent, one has that

$$\alpha=\frac{2-2y}{3-2y}, \tag{13}$$

whereas for those exponents associated with the magnetization and polarization order parameters, one has, respectively,

$$\beta=\frac{2-y}{8(3-2y)} \tag{14}$$

and

$$\beta_p=\frac{1}{4(3-2y)}, \tag{15}$$

where

$$y=\frac{2}{\pi}\cos^{-1}\left\{\frac{1}{2}[\exp(8K_2)-1]\right\}. \tag{16}$$

TABLE II. The critical exponents η and η_p, for several points along the Baxter line of the ferromagnetic Ashkin-Teller model on a square lattice, as computed from the present method. Their corresponding exact values may be calculated from Eqs. (16) and (17) [3], leading to a continuously varying exponent η_p (whose values at the points of interest are presented above) and to $\eta=1/4$ along the whole line.

Point	η (present work)	η_p (present work)	η_p (exact)
I_1	0.2495±0.0028	0.4996±0.0089	$1/2\equiv0.50$
$\tilde{P}$	0.2506±0.0045	0.2504±0.0055	$1/4\equiv0.25$
X_1	0.2497±0.0054	0.3229±0.0078	0.323109…
X_2	0.2479±0.0057	0.3674±0.0067	0.368581…
X_3	0.2510±0.0029	0.4165±0.0089	0.414053…
X_4	0.2509±0.0034	0.4624±0.0064	0.463055…
X_5	0.2528±0.0029	0.5808±0.0095	0.581663…

Using standard scaling relations involving the pair of exponents α and β, as well as α and β_p, one gets that

$$\eta=\frac{1}{4};\quad \eta_p=\frac{1}{2(2-y)}, \tag{17}$$

where η and η_p are the two-point correlation-function critical exponents, associated, respectively, with the magnetization and polarization order parameters. Curiously, the exponent η does not change along the Baxter line, contrary to what happens with its counterpart η_p. The exact values of the exponents above, in the points investigated, are given in Tables II and III.

In the computation of the correlation functions $C^{(1)}(r)$ and $C^{(2)}(r)$, we have approached the investigated points by varying

$$K_1\equiv\left(\frac{J_1}{k_BT_C}\right)\left(\frac{1}{T/T_C}\right)=K_{1C}\left(\frac{1}{T/T_C}\right),$$

$$K_2\equiv\left(\frac{J_2}{k_BT_C}\right)\left(\frac{1}{T/T_C}\right)=K_{2C}\left(\frac{1}{T/T_C}\right), \tag{18}$$

considering small changes around their exact coordinates (K_{1C},K_{2C}) (given in the fourth and fifth columns of Table I, respectively), fluctuating T/T_C around unity, with variations of 0.001.

In the following figures we exhibit our results for one of the points along the Baxter line: namely, point X_2, which lies in between the Potts and Ising points. Initially we will present the results obtained for the smaller linear size—i.e., $L=50$. In this case we compare the results produced by a standard MC simulation, where a single copy of the system is analyzed, with those of the present DS numerical approach. In what concerns correlation functions, our criteria for locating the "critical coordinates" of each point investigated (associated with the finite size of the system considered) consists in searching for the temperature ratios T/T_C at

TABLE III. The critical exponents β and β_p for several points along the Baxter line of the ferromagnetic Ashkin-Teller model on a square lattice, as computed from the present method, are compared quantitatively with the exact values calculated from Eqs. (14)–(16) [3].

Point	β (present work)	β (exact)	β_p (present work)	β_p (exact)
I_1	0.1241±0.0025	$1/8 \equiv 0.125$	0.2489±0.0074	$1/4 \equiv 0.25$
$\tilde{P}$	0.0836±0.0006	$1/12 \equiv 0.08333\ldots$	0.0833±0.0012	$1/12 \equiv 0.083333\ldots$
X_1	0.0924±0.0023	0.092334…	0.1179±0.0021	0.119336…
X_2	0.0986±0.0018	0.098983…	0.1445±0.0035	0.145933…
X_3	0.1060±0.0027	0.106665…	0.1761±0.0026	0.176659…
X_4	0.1157±0.0021	0.116399…	0.2148±0.0017	0.215597…
X_5	0.1484±0.0017	0.149401…	0.3445±0.0034	0.347604…

which the functions $C^{(1)}(r)$ and $C^{(2)}(r)$ present the slowest decay with r. In such cases, one expects the power-law behaviors

$$C^{(1)}(r) \sim r^{-\eta}, \quad C^{(2)}(r) \sim r^{-\eta_p} \quad (r \to \infty). \tag{19}$$

The above power-law behavior is verified for the correlation function $C^{(1)}(r)$ in Fig. 2 where we present the plots of $C^{(1)}(r)$ versus r, in logarithmic scale, with the data obtained from a standard MC simulation and the present DS procedure. The data exhibited corresponds, in each case, to the slowest decay of the correlation function $C^{(1)}(r)$, found from a sweep in T/T_C around its exact value with increments of 0.001, as mentioned above, and using the same simulation parameters for each linear size L (e.g., t_{eq} and t_{av}). In Fig. 2(a) we compare the result of a standard MC simulation with those of the DS technique for a linear size $L=50$; one notices a significant reduction of finite-size effects in the later approach, with respect to the first one, shown through the following features: (i) The ratio T/T_C, associated with the slowest decay of the correlation function $C^{(1)}(r)$, is much closer to the exact result in the DS technique $[(T/T_C)=0.999]$ than in the MC method $[(T/T_C)=0.995]$. (ii) The linear fit, obtained in the log-log plot of the DS results is more reliable in the sense that it covers a larger range of values of r. However, if one restricts the analysis, in each case, to those sets of points associated with the best linear fits, one gets essentially the same estimates (within the error bars) for the exponent η in both techniques—i.e., $\eta=0.2457\pm0.0082$ (linear fit considering five points from MC procedure) and $\eta=0.2492\pm0.0048$ (linear fit with nine points from DS method), in agreement with the well-known exact value ($\eta=1/4$). For increasing values of r, the finite-size effects get pronounced, as expected, leading to points out of the linear regime; this occurs typically for $r>4$ ($r>6$) in the MC (DS) approach. Therefore, for this case, the finite-size effects are weaker in the DS technique, leading to an increase of the order of 50% in the values of r that fit within the power-law behavior of Eq. (19). In Fig. 2(b) we exhibit the DS results for the two linear sizes analyzed, namely, $L=50$ and $L=100$. One observes that this method produces data for the smaller size that are as good as those of the larger size, showing the efficiency of the DS technique, in the sense that one may obtain accurate critical-exponent estimates from rather small lattice sizes; the two estimates for the exponent η, from Fig. 2(b), coincide, within the error bars. Incidentally, in Fig. 2(b) one sees that the $L=50$ data seem to fall in the linear fit even better than those of the linear size $L=100$. We attribute this curious behavior to the following reasons: (i) the size $L=50$ is already sufficient for a good evaluation of critical exponents; (ii) the usual fluctuations near criticality have in some way favored the size $L=50$ in

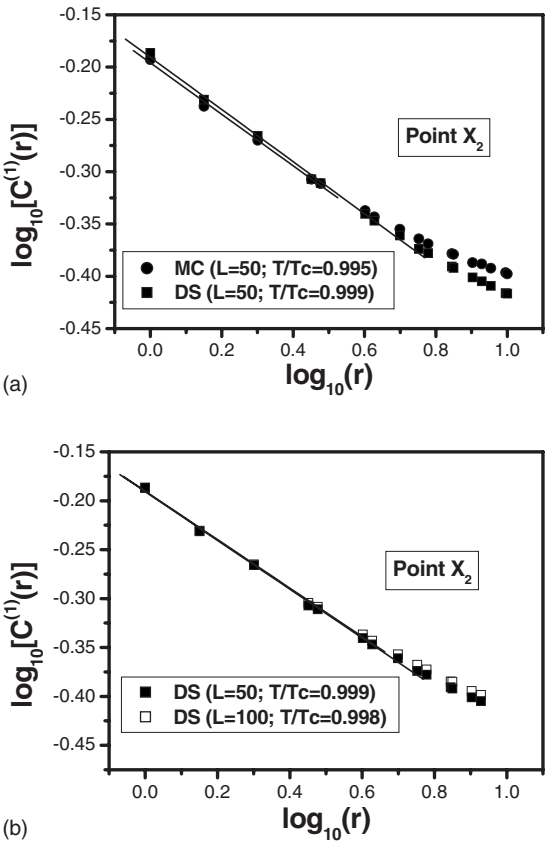

FIG. 2. Linear fits for the computation of the exponent η, associated with the correlation function $C^{(1)}(r)$. (a) The data obtained through standard MC simulations (solid circles) and the present DS approach (solid squares), for a square lattice of linear size $L=50$, are compared. One sees that the finite-size effects are reduced in the latter procedure. (b) Data produced by the present DS approach for the sizes $L=50$ (solid squares) and $L=100$ (open squares).

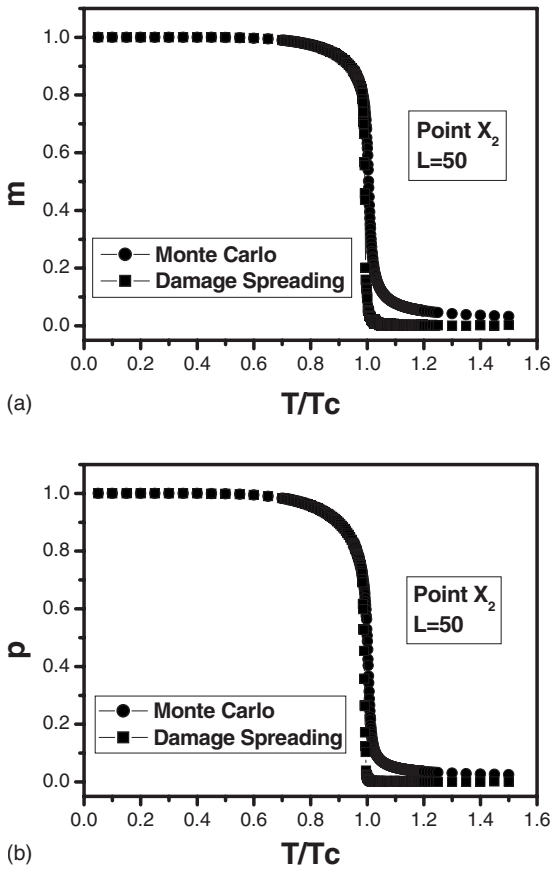

FIG. 3. Comparison of the order parameters of the Ashkin-Teller model [(a) magnetization and (b) polarization] computed through standard MC simulations (solid circles) and the present DS approach (solid squares), for a square lattice of linear size $L=50$. The dimensionless quantity T/T_C changes in such a way that the coordinates K_1 and K_2 [cf. Eq. (18)] vary around the coordinates of the point X_2, given in Table I. One notices a reduction of the finite-size effects in the DS procedure.

the temperature sweep considered in the sense of locating a better estimate for the finite-size critical temperature $T_C(L)$. The slowest decay of the correlation function $C^{(1)}(r)$ occurred at $T/T_C=0.999$ for the linear size $L=50$, in contrast to the value $T/T_C=0.998$ found for the linear size $L=100$; certainly, this later finite-size critical-temperature estimate may be improved and an even slower decay of $C^{(1)}(r)$ could be found in this case for some slightly higher ratio $0.998<(T/T_C)<0.999$, which has probably been missed within the present sweep in temperature.

In Fig. 3 we present the order parameters of the Ashkin-Teller model computed through standard MC simulations and the present DS approach, for a square lattice of linear size $L=50$, using the values of t_{eq} and t_{av} mentioned above in both techniques. Once again, one notices a reduction of the finite-size effects in the DS procedure with respect to the MC method, which produces more pronounced tails in the order parameters for $T>T_C$. The associated critical exponents may be computed through log-log plots of the data exhibited in Fig. 3 in such a way that one gets $\beta=0.0948\pm0.0008$ (MC method) and $\beta=0.0983\pm0.0021$ (DS technique), whereas

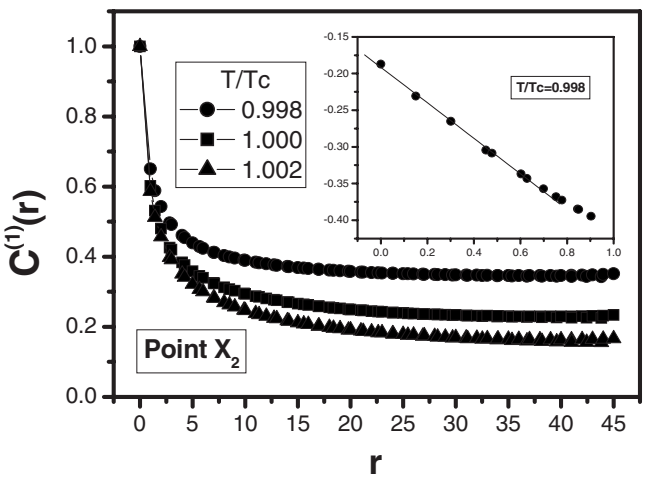

FIG. 4. The correlation function $C^{(1)}(r)$ versus r, for the point X_2, for three typical temperature ratios T/T_C, near criticality. The slowest decay was found for $T/T_C=0.998$, in which case the plot of $\log_{10}[C^{(1)}(r)]$ versus $\log_{10} r$ is presented in the inset, leading to the estimate $\eta=0.2479\pm0.0057$.

$\beta_p=0.1392\pm0.0019$ (MC method) and $\beta_p=0.1412\pm0.0039$ (DS technique). The critical exponents β and β_p, estimated through the DS approach, are in better agreement with the corresponding exact values $\beta=0.098\,983\ldots$ and $\beta_p=0.145\,933\ldots$, than those computed from the MC method.

The efficiency of the present DS approach, and its advantage with respect to standard MC simulations, was illustrated above by comparing data obtained from both methods using the same simulation parameters. Such an improvement is evident for smaller system sizes, like the case analyzed above ($L=50$), for which the finite-size effects are noticeably weaker in the DS technique. From now on, we will restrict ourselves to the results produced by the DS approach for a square lattice of linear size $L=100$.

In Figs. 4 and 5 we show the correlation functions $C^{(1)}(r)$ and $C^{(2)}(r)$ versus r, respectively. For clearness, we present in each case only the correlation functions associated with three typical different ratios T/T_C, including the one of slowest decay, although we have investigated other temperature ratios as well. The power-law behaviors of Eq. (19) are verified in the insets of Figs. 4 and 5, with the associated critical exponents $\eta=0.2479\pm0.0057$ and $\eta_p=0.3674\pm0.0067$, respectively. The relative discrepancies associated with the critical coordinates obtained for the point X_2, when compared with the exact values of Table I, are 0.002 ± 0.001 for K_1 and 0.003 ± 0.001 for K_2. This estimate for the exponent η, considering a square lattice of linear size $L=100$, coincides, within the error bars, with the one obtained for the size $L=50$, described above. This suggests that the linear size $L=100$ is sufficient, at least in what concerns the DS technique, for reliable critical-exponent estimates.

A similar procedure was applied to the other points investigated, and the resulting exponents η and η_p are presented in Table II. Considering the error bars, good agreements with the exact results—within four decimal places—were found. In all cases, the relative discrepancies in our estimates of the critical coordinates, when compared with the exact values

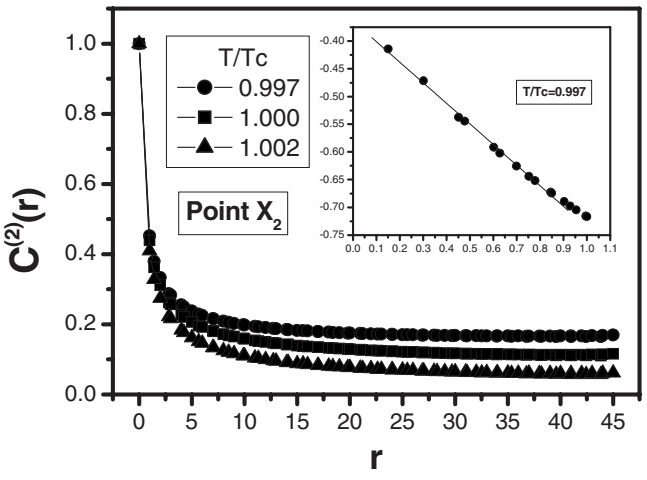

FIG. 5. The correlation function $C^{(2)}(r)$ versus r, for the point X_2, for three typical temperature ratios T/T_C, near criticality. The slowest decay was found for $T/T_C=0.997$, in which case the plot of $\log_{10}[C^{(2)}(r)]$ versus $\log_{10} r$ is presented in the inset, leading to the estimate $\eta_p=0.3674\pm0.0067$.

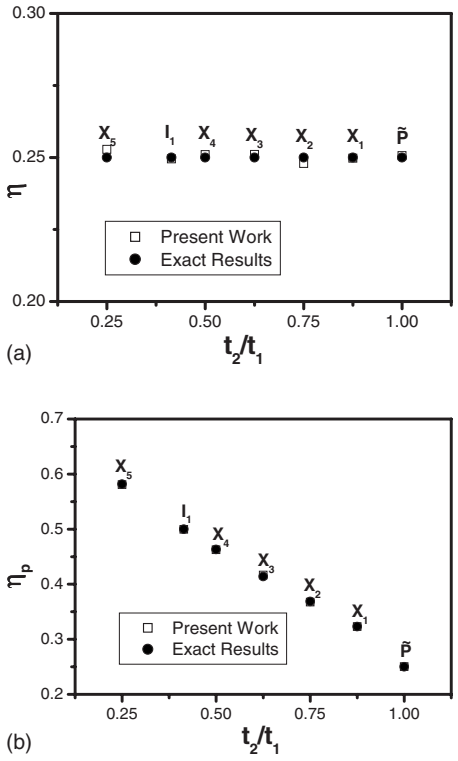

FIG. 6. (a) The critical exponents η, obtained from the present approach (open symbols), are compared qualitatively with the exact value $\eta=1/4$ (solid circles) for the points investigated (represented herein in terms of their corresponding ratio t_2/t_1) along the Baxter line of the ferromagnetic Ashkin-Teller model on a square lattice. (b) The critical exponents η_p, obtained from the present approach (open symbols), are compared qualitatively with the exact values (solid circles) for the same points of case (a). In many cases the symbols appear superposed in such a way that distinctions are not seen clearly.

presented in Table I, were not larger than 0.003 ± 0.001. Such discrepancies are attributed to finite-size effects and are expected to decrease for larger lattice sizes. A comparison of our estimates for the critical exponents η and η_p with the exact results is also presented in Fig. 6, where the investigated points are represented in terms of their corresponding coordinate ratios t_2/t_1. Within such variables, these exponents seem to present a simple dependence on their coordinates; e.g., in Fig. 6(b) one notices that the exponent η_p decreases almost linearly with t_2/t_1 when one moves along the Baxter line from X_5 to the Potts point $(\tilde{P})$, suggesting a smooth and continuous variation in this exponent.

It should be mentioned that, besides accurate estimates of critical exponents, we have detected the well-known universality breakdown along the Baxter line, with our results suggesting smooth and continuous variations of the critical exponents, which represents a nontrivial task within standard Monte Carlo simulations.

In Fig. 7 we exhibit the computed order parameters in terms of the temperature ratio T/T_C, using the evolution of type (III) with the external magnetic field $h=0.0001$. In this case we considered large variations in the coordinates of Eq. (18), with temperature ratios in the interval $T/T_C=0.05,\ldots,1.20$. It is important to mention that similar results could also be achieved for the order parameters m and p by using evolutions of types (I) and (II), respectively, although a much larger computational effort would be required in obtaining their associated curves for such a large temperature range (cf. Ref. [30]). In spite of the reasonably small lattice size considered, one observes whole smooth curves (i.e., characterized by a lack of strong fluctuations)—even near criticality—with weak finite-size effects; this represents one of the greatest advantages of the present DS simulations. From these results, simple log-log plots of the corresponding order parameters versus $\log_{10}(1-T/T_C)$ yielded the associated critical exponents $\beta=0.0986\pm0.0018$ and $\beta_p=0.1445\pm0.0035$ (cf. Table III). These critical-exponent estimates for a square lattice of linear size $L=100$ coincide, within the error bars, with those obtained previously through the DS technique for the size $L=50$. Once again, these results suggest that the linear size $L=100$ is sufficient, at least in what concerns the DS technique, for reliable critical-exponent estimates. Plots similar to those of Fig. 7 were found for the other points investigated, and the corresponding results are presented in Table III. In all cases, the relative discrepancies associated with the computed critical coordinates, when compared with the exact values of Table I, were smaller than, or of the same order as, those obtained through computation of the corresponding correlation functions.

The computed exponents β and β_p are compared quantitatively with the exact results in Table III, where one finds an agreement, within four decimal places, with the exact results (taking into account the error bars). A qualitative comparison of such exponents is presented in Fig. 8, where the investigated points are represented in terms of their corresponding coordinate ratios t_2/t_1. Within such variables, these exponents present smooth monotonically decreasing dependence on their coordinates, as one moves along the Baxter line, from X_5 to the Potts point.

To conclude, we have implemented an effective computational method, for evaluating correlation functions and order

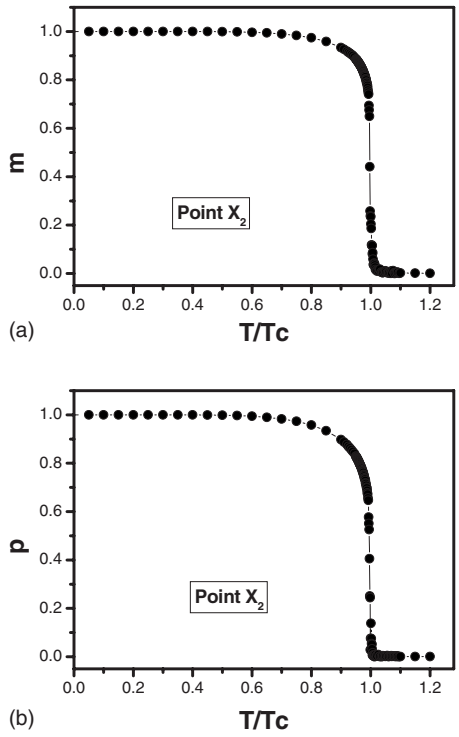

FIG. 7. (a) The order parameters magnetization (a) and polarization (b), for the point X_2, in terms of the temperature ratio T/T_C (solid circles), obtained from the present numerical approach by using the evolution of type (III) (see text). The lines are just guides to the eye.

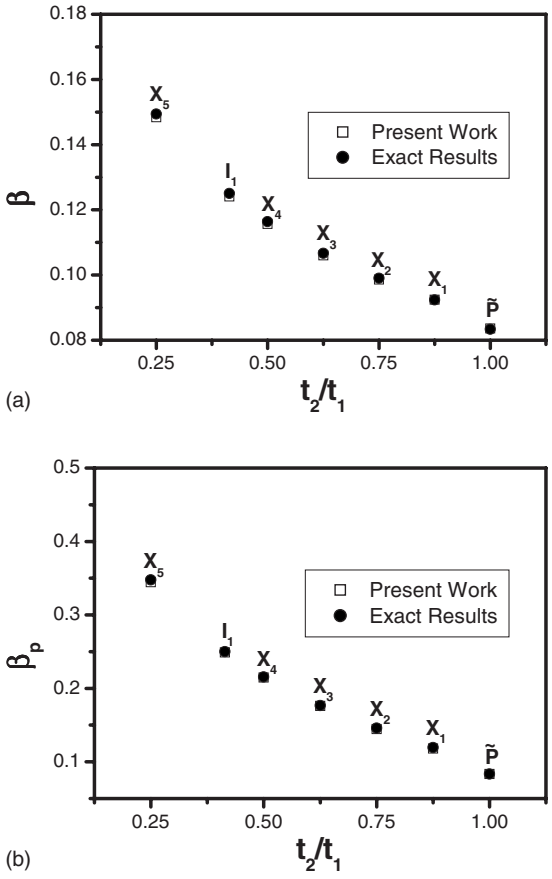

FIG. 8. (a) The critical exponents β (a) and β_p (b), obtained from the present approach (open symbols), are compared qualitatively with the exact values (solid circles) for the points investigated (represented herein in terms of their corresponding ratio t_2/t_1) along the Baxter line of the ferromagnetic Ashkin-Teller model on a square lattice. In many cases the symbols appear superposed in such a way that distinctions are not seen clearly.

parameters in magnetic systems, to the ferromagnetic Ashkin-Teller model on a square lattice. This technique is based on DS simulations and makes use of exact thermodynamic relations derived previously [27], involving computable quantities within DS simulations and two-spin correlation functions, as well as order parameters of the Ashkin-Teller model. The analysis of such quantities was restricted to the Baxter line, well known for its continuously-varying critical exponents. It was shown that the method provides accurate results, in spite of the small lattice sizes considered (larger sizes corresponded to a square lattice of linear size $L=100$), yielding agreement of the computed critical exponents with the corresponding exact results within four decimal places, taking into account the associated error bars. Among such results, one should emphasize those associated with the two-site correlation functions of the present model, which represent hard tasks within standard MC simulations, due to large fluctuations. As far as we know, whole correlation functions and their associated critical exponents, along the Baxter line of the Ashkin-Teller model, have never been calculated numerically in the literature, with a similar precision, and so they are estimated accurately herein within damage-spreading simulations. It should be mentioned that, besides accurate estimates of critical exponents, we have detected the well-known universality breakdown along the Baxter line, with our results suggesting smooth and continuous variations of the critical exponents, which represents a nontrivial task within standard Monte Carlo simulations. The above analysis provides further reliability to this technique, which has already shown its effectiveness on simpler models, like the Ising [26] and Potts [30] two-dimensional ferromagnets, leading to a significant reduction of finite-size effects. The results presented herein encourage application of the method in the study of more complicated open problems in the literature, for which the necessary theoretical background—i.e., the corresponding exact DS relations—has been (or may be) fully elaborated.

ACKNOWLEDGMENTS

Partial financial support from CNPq and Pronex/FAPERJ (Brazilian agencies) is acknowledged.

[1] J. Ashkin and E. Teller, Phys. Rev. **64**, 178 (1943).
[2] R. J. Baxter, Phys. Rev. Lett. **26**, 832 (1971).
[3] R. J. Baxter, *Exactly Solved Models in Statistical Mechanics* (Academic Press, London, 1982).
[4] F. Y. Wu and K. Y. Lin, J. Phys. C **7**, L181 (1974).
[5] I. G. Enting, J. Phys. A **8**, 1681 (1975).
[6] M. P. M. den Nijs, J. Phys. A **12**, 1857 (1979).
[7] M. Kohmoto, M. P. M. den Nijs, and L. P. Kadanoff, Phys. Rev. B **24**, 5229 (1981).
[8] J. R. Drugowich de Felício, R. Koberle, and L. N. de Oliveira, J. Phys. C **15**, L773 (1982).
[9] A. M. Mariz, C. Tsallis, and P. Fulco, Phys. Rev. B **32**, 6055 (1985).
[10] S. Wiseman and E. Domany, Phys. Rev. E **48**, 4080 (1993).
[11] B. Nienhuis, in *Phase Transitions and Critical Phenomena*, edited by C. Domb and J. L. Lebowitz (Academic Press, New York, 1987), Vol. 11.
[12] H. Gould and J. Tobochnik, *An Introduction to Computer Simulation Methods*, 2nd ed. (Addison-Wesley, Reading, MA, 1996).
[13] K. Binder and D. W. Heermann, *Monte Carlo Simulation in Statistical Physics* (Springer-Verlag, Berlin, 1988).
[14] D. P. Landau and K. Binder, *A Guide to Monte Carlo Simulations in Statistical Physics* (Cambridge University Press, Cambridge, England, 2000).
[15] H. E. Stanley, D. Stauffer, J. Kertész, and H. J. Herrmann, Phys. Rev. Lett. **59**, 2326 (1987).
[16] B. Derrida and G. Weisbuch, Europhys. Lett. **4**, 657 (1987).
[17] U. M. S. Costa, J. Phys. A **20**, L583 (1987).
[18] G. Le Caër, J. Phys. A **22**, L647 (1989).
[19] P. Grassberger, J. Phys. A **28**, L67 (1995).
[20] A. M. Mariz, H. J. Herrmann, and L. de Arcangelis, J. Stat. Phys. **59**, 1043 (1990).
[21] F. D. Nobre, A. M. Mariz, and E. S. Sousa, Phys. Rev. Lett. **69**, 13 (1992).
[22] M. F. de A. Bibiano, F. G. Brady Moreira, and A. M. Mariz, Phys. Rev. E **55**, 1448 (1997).
[23] L. da Silva, F. A. Tamarit, and A. C. N. Magalhães, J. Phys. A **30**, 2329 (1997).
[24] E. M. de Sousa Luz, M. P. Almeida, U. M. S. Costa, and M. L. Lyra, Physica A **282**, 176 (2000).
[25] J. A. Redinz, F. A. Tamarit, and A. C. N. Magalhães, Physica A **293**, 508 (2001).
[26] A. Coniglio, L. de Arcangelis, H. J. Herrmann, and N. Jan, Europhys. Lett. **8**, 315 (1989).
[27] A. M. Mariz, J. Phys. A **23**, 979 (1990).
[28] A. M. Mariz, A. M. C. de Souza, and C. Tsallis, J. Phys. A **26**, L1007 (1993).
[29] A. M. Mariz, E. S. de Sousa, and F. D. Nobre, Physica A **257**, 429 (1998).
[30] A. S. Anjos, D. A. Moreira, A. M. Mariz, and F. D. Nobre, Phys. Rev. E **74**, 016703 (2006).